Rapid Communications

Asymmetry profiles of the fragment anisotropy parameters along the Fano resonances in the photodissociation of H_2

Jie Wang[1,2] and Yuxiang Mo[1,*]

[1]*Department of Physics and State Key Laboratory of Low-Dimensional Quantum Physics, Tsinghua University, Beijing 100084, China*

[2]*National Innovation Institute of Defense Technology, Academy of Military Sciences of People's Liberation Army of China, Beijing 100071, China*

(Received 25 September 2020; accepted 9 November 2020; published 25 November 2020)

The anisotropy parameters (β) of photofragments near a Fano resonance vary with the excitation energies. We call the curve describing such a relationship the β profile. In this Rapid Communication, we report measurements of the β profiles for the H($2l$) and D($2l$) fragments along six Fano resonances in the predissociation of H_2 and D_2 near the second dissociation threshold. In contrast to a previous theoretical prediction, the measured β profiles are found to be asymmetric. An analytical expression of the β profile was derived based on the Fano formula and was used to fit the measured β profiles. The β profiles are found to be more sensitive than the Fano profiles to the Fano q parameters, as well as to the intensity ratios between the interacting and noninteracting continuum states. The β values due to the resonance state, the continuum state, and the interference between the resonance and the continuum states in the Fano resonance were also determined. The β profile should not only provide us with a tool to measure the parameters characterizing the Fano resonance, but also help gain further physical insight into the Fano resonances.

DOI: 10.1103/PhysRevA.102.050803

Introduction. Resonance involving a discrete state embedded in a continuum is ubiquitous in physics [1–3]. Such a discrete-continuum interaction is often called a Fano resonance. For photoexcitation to such mixed discrete and continuum states, the absorption cross sections as a function of excitation photon energies would display an asymmetric line profile due to the interference between the two types of states. The asymmetric profile is usually referred to as the Fano profile or Beutler-Fano profile [3,4]. Fano profiles provide information about the coupling strength between the discrete and continuum states, as well as about the relative optical transition intensities to the bound and to the continuum states. Fano profiles are thus crucial for the understanding of the excitation spectra in atomic and molecular systems as well as in solid state physics [1–6].

The physics underlying the Fano profiles has been attracting a great number of experimental and theoretical studies [7–10]. Most of them have focused on the spectral properties of the profiles. The decay dynamics along the Fano profiles, however, have not been paid much attention, for example, the angular distributions of the photofragments.

The variation of the fragment angular distributions across a Fano resonance in molecular photodissociation is very interesting because the angular distributions are sensitive to the photoexcitation dynamics and the details of the state mixing [5,11–18]. In this Rapid Communication, the spotlight is on the angular distributions of the H($2l$) and D($2l$) fragments along the Fano resonances of H_2 and D_2 in the second threshold region. This choice takes advantage of the fact that the predissociations in this energy region have been studied in great detail both theoretically and experimentally and can be simplified as one isolated resonance interacting with only one continuum [19–36]. Those resonances are also known as Feshbach resonances.

Here, we report measurements of the fragment anisotropy parameters as a function of excitation energies across six Fano resonances in the predissociation of H_2 and D_2. We plotted the results and refer to the curves as β profiles. Our β profiles are found to be asymmetric and sensitive to the parameters characterizing the Fano profiles. The β profiles may thus provide us with a tool to study the Fano resonances.

Experiment. Our experimental setup consists of a tunable XUV laser pump (83.7–84.2 nm, ~10 nJ/pulse), a UV laser probe system (365 nm, 1 mJ/pulse), and a typical velocity map imaging apparatus [14,32–36]. The XUV laser was generated by resonance-enhanced four-wave sum mixing ($2\omega_1 + \omega_2$) in a pulsed Kr jet using two laser beams. The first laser beam with frequency ω_1 was generated by the frequency tripling of a dye laser, and the $2\omega_1$ was equal to the transition frequency of the krypton of $4p^5(^2P_{1/2})5p[1/2]_0 \leftarrow (4p^6)\,^1S_0$ (98 855.1 cm^{-1}). The second laser beam (ω_2) was tuned from 487 to 502 nm. The two dye lasers were pumped by an Nd:YAG laser (repetition rate 20 Hz). The probe UV laser ionizing the H($2l$) or D($2l$) fragments was from the frequency doubling of a third dye laser pumped by the second Nd: YAG laser.

Angular distribution. The angular distribution of the photofragments can be determined from the velocity map images and are fitted using the well-known formula [37]

$$f(\theta) \propto 1 + \beta P_2(\cos\theta), \tag{1}$$

*Corresponding author: ymo@mail.tsinghua.edu.cn

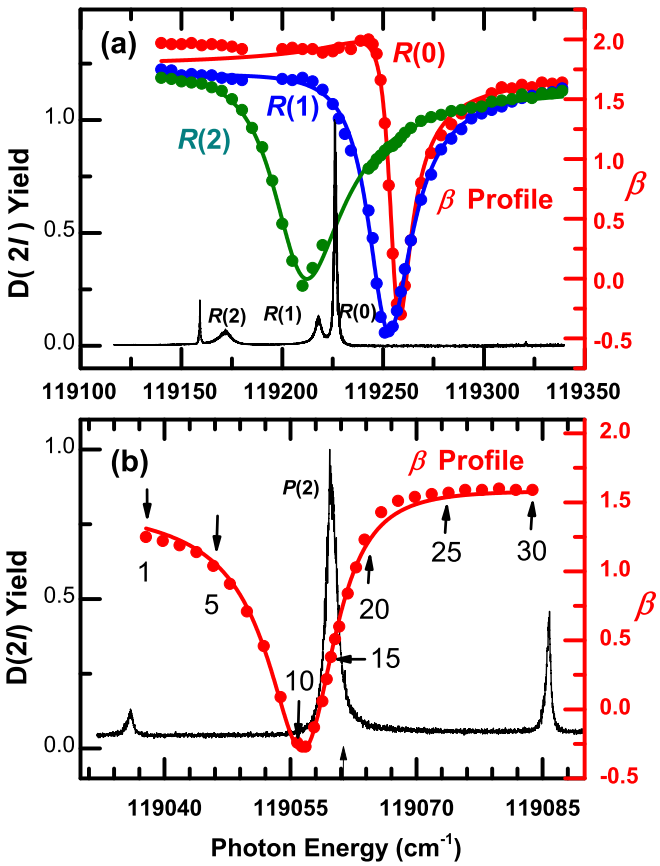

FIG. 1. The anisotropy parameters β of the D($2l$) fragments as a function of excitation photon energies, called β profiles, for the predissociation of D_2 in the rotational branches of (a) $R(0)$, $R(1)$, $R(2)$, and (b) $P(2)$ of the $3p\pi D\,^1\Pi_u(\upsilon = 4) \leftarrow X\,^1\Sigma_g^+(\upsilon = 0)$ transition. The corresponding normalized D($2l$) fragment yield spectra from Ref. [33] are also shown. For the β profiles, the solid dots denote the experimental data, whereas the continuous lines result from the fits using Eq. (5). See Table I for the fitting parameters. Using the index numbers in (b) along the β profiles, the velocity map images and the corresponding angular distributions can be found in Fig. 3.

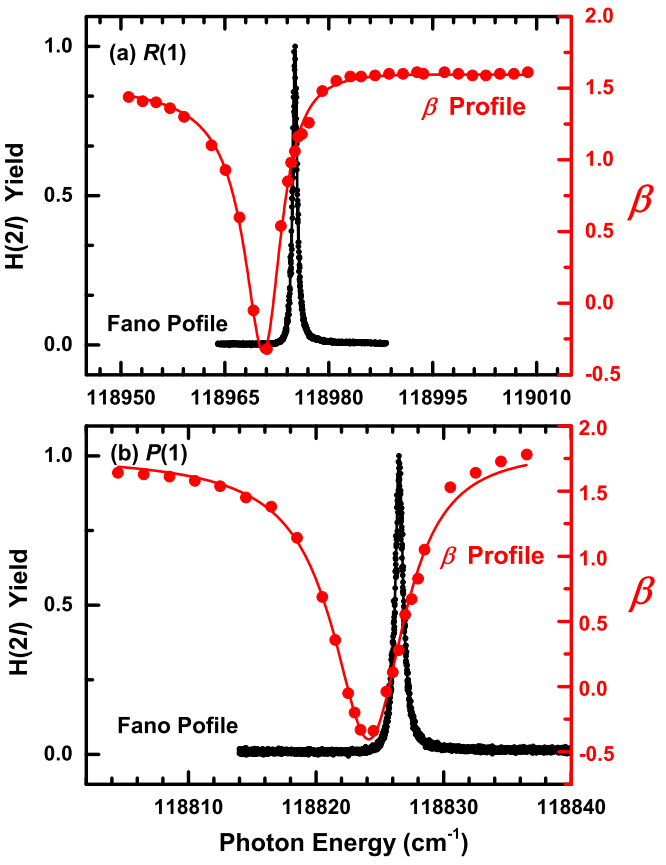

FIG. 2. See caption of Fig. 1. The β profiles for the predissociation of H_2 in the rotational branches of (a) $R(1)$ and (b) $P(1)$, of the $4p\sigma B''\Sigma_u^+(\upsilon = 1) \leftarrow X\,^1\Sigma_g^+(\upsilon = 0)$ transition. The normalized H($2l$) fragment yield spectra are taken from Ref. [32].

where θ is the angle between the recoil velocity vector and the polarization direction of the dissociation laser, and $P_2(\cos\theta)$ is the second-order Legendre polynomial. β is the so-called anisotropy parameter. For direct photodissociation, β has a limiting value of 2 or -1, corresponding to a parallel or a perpendicular transition, respectively. For a predissociation occurring right at the resonance center of the Fano profile, β may be calculated using theoretical models under the assumption of a definite final angular momentum of the parent molecule [11,17,32].

Experimental results. We have measured the rotationally resolved angular distributions along the Fano profiles for the $R(0)$, $R(1)$, $R(2)$, and $P(2)$ branches of the vibrational bands $3p\pi D\,^1\Pi_u(\upsilon = 4) \leftarrow X\,^1\Sigma_g^+(\upsilon = 0)$ of D_2, and for the $R(1)$ and $P(1)$ branches of the $4p\sigma B''\,\Sigma_u^+(\upsilon = 1) \leftarrow X\,^1\Sigma_g^+(\upsilon = 0)$ transition of H_2. The corresponding β profiles are shown in Figs. 1 and 2, respectively. To observe the relationships between the Fano and the β profiles, the corresponding D($2l$) and H($2l$) fragment yield spectra published previously are also shown in Figs. 1 and 2, respectively [32,33]. Figure 3 shows examples of the rotationally resolved velocity map images and the angular distributions of the D($2l$) fragments along the Fano profiles of the $P(2)$ branch of the $3p\pi D\,^1\Pi_u(\upsilon = 4) \leftarrow X\,^1\Sigma_g^+(\upsilon = 0)$ transition. The corresponding measurements for other transitions can be found in the Supplemental Material [38].

The β profiles shown in Figs. 1 and 2 are all asymmetric with respect to the minima of the β values, which is in contrast with a previous theoretical prediction [13]. This asymmetry can be reproduced by an analytical expression derived from the Fano formula.

β-profile formula. The asymmetric Fano profile can be described by the so-called Fano formula [3,6],

$$\sigma(\varepsilon) = \sigma_{ic}\frac{(q+\varepsilon)^2}{1+\varepsilon^2} + \sigma_{nc}, \quad \varepsilon = \frac{2(\omega-\omega_0)}{\Gamma}, \tag{2}$$

where q is the Fano parameter, ε the reduced energy, ω_0 the resonance center, and Γ the linewidth of the line profile. σ_{ic} and σ_{nc} represent the partial absorption cross sections due to the continuum states interacting and noninteracting with the discrete state, respectively. The total absorption cross section can be decomposed into three parts [1,3,9,11–13],

$$\begin{aligned}\sigma(\varepsilon) &= \frac{q^2-1}{\varepsilon^2+1}\sigma_{ic} + \frac{2q\varepsilon}{\varepsilon^2+1}\sigma_{ic} + (\sigma_{ic}+\sigma_{nc}) \\ &= \sigma_{\rm res} + \sigma_{\rm int} + \sigma_c,\end{aligned} \tag{3}$$

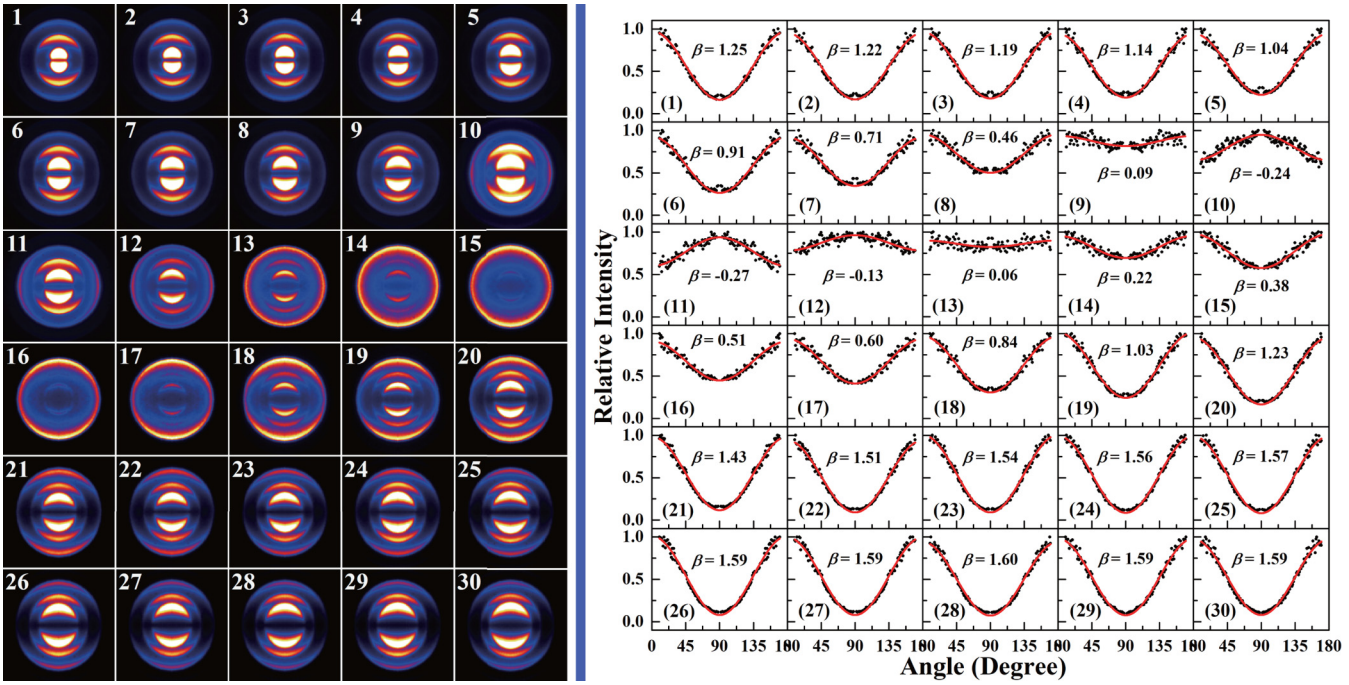

FIG. 3. Rotationally resolved velocity map images (left panel), and the corresponding angular distributions (right panel), of the D($2l$) fragments in the $P(2)$ branch of the $3p\pi D\,^1\Pi_u^+(\upsilon = 4) \leftarrow X\,^1\Sigma_g^+(\upsilon'' = 0)$ transition from the predissociation of D_2. In the images (left panel), there are three rings due to the transitions starting from the initial angular momenta of $J'' = 0$, 1, and 2, respectively. The angular distributions (right panel) are for $J'' = 2$, i.e., the outer rings in the images. In the panels of fragment angular distributions, the dots are the experimental data and the continuous lines are the fits using Eq. (1). The determined β values are used to plot the β profile in Fig. 1(b).

where $\sigma_{\rm res}$, $\sigma_{\rm int}$, and σ_c represent the partial absorption cross sections due to the discrete state, interference between the discrete and continuum states, and the continuum state, respectively. The Fano formula is very general and can be derived using various formalisms [3,6,11]. For the differential cross sections of the photofragments, the above equation can be rewritten as [11–13]

$$\sigma(\varepsilon,\theta) = \frac{1}{4\pi}\left[\frac{q^2-1}{\varepsilon^2+1}[1+\beta_{\rm res}P_2(\cos\theta)]\sigma_{ic} + \frac{2q\varepsilon}{\varepsilon^2+1}[1+\beta_{\rm int}P_2(\cos\theta)]\sigma_{ic} + (\sigma_{ic}+\sigma_{nc})[1+\beta_c P_2(\cos\theta)]\right], \tag{4}$$

where $\beta_{\rm res}$ is the fragment anisotropy parameter due to the dissociation of the discrete (resonance) state, β_c is due to the continuum state, and $\beta_{\rm int}$ is due to the interference between the discrete state and the continuum state. An integration of the spherical angles in Eq. (4) results in Eq. (2), as required.

Rewriting Eq. (4) in the form of Eq. (1), we obtain

$$\beta = \frac{\beta_{\rm res}(q^2-1)\gamma + 2q\varepsilon\beta_{\rm int}\gamma + (\varepsilon^2+1)\beta_c}{(\varepsilon+q\gamma)^2 + (1-\gamma)(1+\gamma q^2)}, \qquad \gamma = \frac{\sigma_{ic}}{\sigma_{ic}+\sigma_{nc}}, \tag{5}$$

where γ is the fraction of the absorption cross section of the interacting continuum relative to that of the total continuum. If $\beta_{\rm res} \neq \beta_{\rm int}$, Eq. (5) results in an asymmetric β profile. In the case of $\beta_{\rm res} = \beta_{\rm int}$, Eq. (5) yields a symmetric profile published earlier, which was derived based on a combination of the Fano formula and a perturbative quantum treatment of diatomic predissociation [11–13].

Assuming that there is no coupling between the rotational angular momenta of the fragments and the orbital angular momenta of the fragments, the γ in Eq. (5) was shown to be [13]

$$\gamma = (2J_c+1)\begin{pmatrix} J_c & 1 & J_i \\ |\Omega_c| & |\Omega_i|-|\Omega_c| & -|\Omega_i| \end{pmatrix}^2, \tag{6}$$

where J_i represents the rotational angular momentum of the ground state, and J_c stands for the excited continuum state interacting with the discrete state. Ω_i and Ω_c are the projections of J_i and J_c on the diatomic molecular axis, respectively.

It is interesting to note that Eq. (4) predicts that the angle-resolved line profiles should not have the exact Fano line shapes, even though they can still be fitted approximately with the Fano formula. In this case, the q parameters are dependent on θ, which is found to be true in the predissociation of H_2 [14].

q parameter. We have fitted the measured β profiles shown in Figs. 1 and 2 to Eq. (5) by using the nonlinear least-squares method. The fitting parameters are listed in Table I. In the fits, the reduced energies ε were calculated using the published

TABLE I. Parameters in the β profiles [Eq. (5)] and in the Fano profiles [Eq. (2)], as determined from fitting the experimental data. The numbers in parentheses are the uncertainties of the last digits.

	β profile						Fano profile[b]		
Branch	β_{res}	β_c	β_{int}	γ	q	Theory γ[a]	q	Γ	ω_0
				$D_2[3p\pi D\,^1\Pi_u(\upsilon=4) \leftarrow X\,^1\Sigma_g^+(\upsilon=0)]$					
$R(0)$	1.97(2)	1.75(1)	2.00(2)	0.88(1)	−33.8(4)	1.0	−40(10)	1.16(15)	119238.8(3)
$R(1)$	1.30(2)	1.67(1)	1.84(2)	0.71(1)	−17.0(1)	0.67	−22(6)	3.38(15)	129231.0(3)
$R(2)$	1.07(2)	1.66(1)	2.00(3)	0.44(2)	−12.7(2)	0.60	−12(3)	6.54(15)	119189.9(3)
$P(2)$	0.39(2)	1.54(2)	2.00(6)	0.24(2)	18.5(8)	0.40	18(3)	1.22(15)	119059.8(3)
				$H_2[4p\sigma B''\Sigma_u^+(\upsilon=1) \leftarrow X\,^1\Sigma_g^+(\upsilon=0)]$					
$R(1)$	1.08(1)	1.57(1)	1.74(1)	0.62(1)	20.0(3)	0.67	30(12)[c]	0.67(3)[c]	118975.1(5)
$P(1)$	0.33(2)	1.79(3)	2.00(7)	0.29(2)	22.6(12)	0.33	30(12)[c]	0.67(3)[c]	118826.5(5)

[a]Calculated using Eq. (6).
[b]From Refs. [32,33]. The units of Γ and ω_0 are in cm^{-1}.
[c]Improved results derived from the spectra in Ref. [32].

resonance centers (ω_0) and linewidths (Γ) that are also listed in Table I [32,33].

It is seen that the fitted curves reproduce the asymmetric line shapes of the β profiles. The q parameters determined from fitting the β profiles are in good agreement with those from fitting the Fano profiles [24,28,32,33], yet, the former have much smaller uncertainties. The larger uncertainties of the q parameters obtained from fitting the Fano profiles arise mainly from three reasons. First, for $|q|$ values larger than 10, the line shapes are not very sensitive to q [39]. Second, different transitions may overlap (see Fig. 1). Third, it is usually assumed that background signals are zero [$\sigma_{nc}=0$ in Eq. (2)]. By fitting the β profiles with the rotationally resolved anisotropy parameters, these drawbacks can be overcome. Therefore, fitting the β profiles may provide a more accurate method to determine the Fano q parameters than by fitting the Fano profiles themselves.

It is interesting to find that the β profiles are much broader than those of the corresponding Fano profiles, as seen in Figs. 1 and 2. The following facts may provide some reasons for this: (a) The linewidth of the Fano profile is determined by the squares of the interaction strength between the discrete and the continuum state [3,5], however, (b) the β parameter is determined by the electronic symmetry of the continuum state, as well as by the mixing ratio between the continuum and the discrete states [11]. Obviously, more detailed studies are needed to understand the widths of the β profiles. It is also worth noting that similar phenomena have been found in the rovibrational autoionization of H_2, as reported in a previous theoretical study [40].

The predissociation mechanism of D_2 in the $3p\pi D\,^1\Pi_u$ states is well known [19–31], which is due to the rotational-electronic $(J\cdot l)$ coupling between the $3p\pi D\,^1\Pi_u^+$ and the $3p\sigma B'\,^1\Sigma_u^+$ states. Based on this model, it is easy to derive the following ratios [24,33]: $q[R(0)]:q[R(1)]:q[R(2)]=1:1/2:1/3$, and $q[R(0)]:q[P(2)]=-2$. As seen in Table I, the q values of D_2 obtained by fitting the β profiles approximately reproduce the above relationships, which supports the validity of Eq. (5).

For the predissociation of H_2 in the $4p\sigma B''\,\Sigma_u^+(\upsilon'=1)$ state, the dissociation mechanism involves the vibronic coupling between the $4p\sigma B''\,\Sigma_u^+$ and the $3p\sigma B'\,^1\Sigma_u^+$ states [24,27]. The q values are thus not expected to display a dependency on the rotational branches, which is supported by the measured values (see Table I).

γ parameter. As seen in Table I, the γ parameters for H_2, determined from the fitting, are in good agreement with those calculated using Eq. (6). Conversely, for D_2 the determined γ parameters are only in qualitative agreement with the calculations. As we mentioned, the predissociation of the $4p\sigma B''\,\Sigma_u^+(\upsilon'=1)$ state is due to vibronic coupling, and that of the $3p\pi D\,^1\Pi_u^+$ state is due to rotational-electronic coupling. However, the γ parameters as calculated by Eq. (6) are not dependent on the predissociation mechanisms [13]. Our experimental results may suggest that future theoretical calculations of the γ parameters should take the predissociation mechanism into consideration.

The γ parameters are difficult to measure. As we described above, in the fitting of the Fano profiles, it usually assumes that the background signals are zero, that is, $\gamma=1$. To the best of our knowledge, few experiments have reported the γ parameters even though they are important to characterize the theoretical calculations [30]. The β profile thus provides us with a valuable tool to measure the γ parameters, which in turn might be instrumental to test the validity of theoretical models dealing with discrete-continuum state interactions.

Anisotropy parameter. The anisotropy parameters β_{int}, β_{res}, and β_c were also determined and are shown in Table I. The β_{res} values at the line centers are in good agreement with previous measurements [32,33]. The β_c values are consistent with parallel transitions. The β_{int} values are almost 2, in agreement with the theoretical predictions [11]. It is seen in Table I that $\beta_c<\beta_{int}$, and this is what leads to asymmetric β profiles, as mentioned above.

It is also interesting to point out that the observed minima of the β profiles are neither at the energy positions of the resonance centers ($\omega=\omega_0$ or $\varepsilon=0$) nor are they at the minima of the Fano profiles ($\omega=\omega_0-q\Gamma/2$ or $\varepsilon=-q$). If we assume $\beta_c=\beta_{int}$, which is approximately true in our measured transitions, the minimum of the β profile is at $\omega=\omega_0-\gamma q\Gamma/2$ or $\varepsilon=-\gamma q$, as can be derived from Eq. (5) [13]. Because γ is a positive fraction number, the minimum of the β profile is thus

located somewhere between the peak of the Fano resonance and the minimum of the Fano profile, which agrees with the measured results shown in Figs. 1 and 2.

Summary. We have measured the anisotropy parameters of the photofragments H($2l$) and D($2l$) along six Fano resonances in the photodissociation of H_2/D_2 near the second dissociation threshold. We refer to them as β profiles. All the β profiles are found to be asymmetric and include contributions from the resonance state, the continuum state, as well as from the interference between the continuum and resonance states. The β-profile method should not only provide us with a sensitive and accurate method to obtain the Fano q parameters, and the ratio of cross sections between the interacting and noninteracting continua, but also different physical insights into the Fano resonances.

We are grateful to Dr. Gabriel J. Vázquez of Universidad Nacional Autonóma de México for carefully reading the manuscript and making valuable suggestions. This work is funded by Projects No. 21833003 and No. 21773134, supported by the National Science Foundation of China, and by Grant No. 2018YFA0306504, supported by the National Key R&D Program of China.

[1] A. E. Miroshnichenko, S. Flach, and Y. S. Kivshar, Fano resonances in nanoscale structures, Rev. Mod. Phys. **82**, 2257 (2010).

[2] J. Li, W.-D. Schneider, R. Berndt, and B. Delley, Kondo Scattering Observed at Single Magnetic Impurity, Phys. Rev. Lett. **80**, 2893 (1998).

[3] U. Fano, Effects of configuration interaction on intensities and phase shifts, Phys. Rev. **124**, 1866 (1961).

[4] H. Beutler, A. Deubner, and H.-O. Jünger, Über das absorptionsspektrum des wasserstoffs. II, Z. Phys. **98**, 181 (1935).

[5] H. Lefebvre-Brion and R. W. Field, *The Spectra and Dynamics of Diatomic Molecules: Revised and Enlarged Edition* (Academic, New York, 2004).

[6] H. Friedrich, *Scattering Theory* (Springer, Berlin, 2016).

[7] M. Wickenhauser, J. Burgdörfer, F. Krausz, and M. Drescher, Time Resolved Fano Resonances, Phys. Rev. Lett. **94**, 023002 (2005).

[8] C. Ott, A. Kaldun, P. Raith, K. Meyer, M. Laux, J. Evers, C. H. Keitel, C. H. Greene, and T. Pfeifer, Lorentz meets Fano in spectral line shapes: A universal phase and its laser control, Science **340**, 716 (2013).

[9] V. Gruson *et al.*, Attosecond dynamics through a Fano resonance: Monitoring the birth of a photoelectron, Science **354**, 734 (2016).

[10] A. Kaldun *et al.* Observing the ultrafast buildup of a Fano resonance in the time domain, Science **354**, 738 (2016).

[11] M. Glass-Maujean and L. D. A. Siebbeles, Angular distribution of photofragments along a Fano profile, Phys. Rev. A **44**, 1577 (1991).

[12] L. D. A. Siebbeles, J. M. Schins, J. Los, and M. Glass-Maujean, Resonance of the $j^3\Delta_g$ state in the differential photodissociation cross section of H_2, Phys. Rev. A **44**, 1584 (1991).

[13] L. D. A. Siebbeles and M. Glass-Maujean, Polarization of atomic photofragment fluorescence for excitation along a Fano profile: A quantum-mechanical study, J. Chem. Phys. **101**, 1019 (1994).

[14] Q. Meng, J. Wang, and Y. Mo, Angle-resolved Beutler-Fano profile and dynamics for the predissociation of H_2, Phys. Rev. A **93**, 050501(R) (2016).

[15] S. Lee, Quantum mechanical analysis of photofragment alignment near asymmetric resonances, J. Chem. Phys. **105**, 10782 (1996).

[16] S. Lee, H. Sun, B. Kim, and K. F. Freed, Vector properties of $S(^3P)$ and $S(^1D)$ the photodissociation of SH: Quantum interference and overlapping resonance, J. Chem. Phys. **116**, 10656 (2002).

[17] H. Kim, K. S. Dooley, S. W. North, G. E. Hall, and P. L. Houston, Anisotropy of photofragment recoil as a function of dissociation lifetime, excitation frequency, rotational level, and rotational constant, J. Chem. Phys. **125**, 133316 (2006).

[18] A. Knie, M. Patanen, A. Hans, I. D. Petrov, J. D. Bozek, A. Ehresmann, and Ph. V. Demekhin, Angle-Resolved Auger Spectroscopy as a Sensitive Access to Vibronic Coupling, Phys. Rev. Lett. **116**, 193002 (2016).

[19] F. J. Comes and G. Schumpe, Einfluß der Rotation auf die Lebensdauer Prädissoziierender Moleküle, Z. Naturforsch. A **26**, 538 (1971).

[20] G. Herzberg, *Topics in Modern Physics: A Tribute to Edward U. Condon* (Colorado Associated University Press, Boulder, CO, 1971), p.191.

[21] P. Borrell, P. M. Guyon, and M. Glass-Maujean, H_2 and D_2 photon impact predissociation, J. Chem. Phys. **66**, 818 (1977).

[22] M. Glass-Maujean, J. Breton, and P. M. Guyon, A Fano-profile study of the predissociation of the $3p\pi D\,^1\Pi_u^+$ state of H_2, Chem. Phys. Lett. **63**, 591 (1979).

[23] P. M. Dehmer and W. A. Chupka, Predissociation of the $3p\pi D\,^1\Pi_u^+$ state in H_2, HD, and D_2, Chem. Phys. Lett. **70**, 127 (1980).

[24] M. Rothschild, H. Egger, R. T. Hawkins, J. Bokor, H. Pummer, and C. K. Rhodes, High-resolution spectroscopy of molecular hydrogen in the extreme ultraviolet region, Phys. Rev. A **23**, 206 (1981).

[25] F. Mrugała, Predissociation of the $D\,^1\Pi_u^+$ state of H_2 by photon impact, Mol. Phys. **65**, 377 (1988).

[26] H. Gao, C. Jungen, and C. H. Greene, Predissociation of H_2 in the $3p\pi D\,^1\Pi_u^+$ state, Phys. Rev. A **47**, 4877 (1993).

[27] H. Gao, Predissociation of H_2 in the Rydberg states, J. Chem. Phys. **107**, 7278 (1997).

[28] G. D. Dickenson *et al.*, VUV spectroscopic study of the $D\,^1\Pi_u$ state of molecular deuterium, Mol. Phys. **109**, 2693 (2011).

[29] M. Glass-Maujean, H. Schmoranzer, C. Jungen, I. Haar, A. Knie, P. Reiss, and A. Ehresmann, *Ab initio* nonadiabatic study of the $3p\pi D\,^1\Pi_u^+$ state of H_2 and D_2, Phys. Rev. A **86**, 052507 (2012).

[30] J. Zs. Mezei, I. F. Schneider, M. Glass-Maujean, and C. Jungen, Resonances in photoabsorption: Predissociation line shapes in the $3p\pi D\,^1\Pi_u^+ \leftarrow X\,^1\Sigma_g^+$ system in H_2, J. Chem. Phys. **141**, 064305 (2014).

[31] J. Zs. Mezei, I. F. Schneider, and Ch. Jungen, Multichannel quantum defect theory of photodissociation of H_2, EPJ Web Conf. **84**, 04005 (2015).

[32] Q. Meng and Y. Mo, Predissociation dynamics in the $3p\pi D\,^1\Pi_u^{\pm}(\upsilon = 3)$ and $4p\sigma B''\,^1\Sigma_u^{+}(\upsilon = 1)$ states of H_2 revealed by product branching ratios and fragment angular distributions, J. Chem. Phys. **144**, 154305 (2016).

[33] J. Wang, Q. Meng, and Y. Mo, Electronic and Tunneling predissociations in the $2p\pi C\,^1\Pi_u^{\pm}(\upsilon = 19)$ and $3p\pi D\,^1\Pi_u^{\pm}(\upsilon = 4, 5)$ states of D_2 studied by a combination of XUV laser and velocity map imaging, J. Phys. Chem. A **121**, 5785 (2017).

[34] J. Wang and Y. Mo, Isotope effect and gerade versus ungerade symmetry in HD predissociation revealed by the $H(2s)$, $H(2p)$, $D(2s)$, and $D(2p)$ fragments, Phys. Rev. A **98**, 062509 (2018).

[35] J. Wang, Q. Meng, and Y. Mo, Oscillation of Branching Ratios between the $D(2s) + D(1s)$ and the $D(2p) + D(1s)$ Channels in Direct Photodissociation of D_2, Phys. Rev. Lett. **119**, 053002 (2017).

[36] J. Wang and Y. Mo, Predissociation dynamics of $D_2 + h\upsilon \rightarrow D(1s_{1/2}) + D(2p_{1/2,3/2,}2s_{1/2})$ revealed by the spin-orbit state resolved fragment branching ratios and angular distributions, J. Chem. Phys. **150**, 144306 (2019).

[37] R. N. Zare and D. R. Herschbach, Doppler line shape of atomic fluorescence excited by molecular photodissociation, Proc. IEEE **51**, 173 (1963).

[38] See Supplemental Material at http://link.aps.org/supplemental/10.1103/PhysRevA.102.050803 for tables listing all the anisotropy parameters and the corresponding fragment velocity map images.

[39] S. Meierott, T. Hotz, N. Néel, and J. Kröger, Asymmetry parameter of peaked Fano line shapes, Rev. Sci. Instrum. **87**, 103901 (2016).

[40] M. Raoult, Ch. Jungen, and D. Dill, Photoelectron angular distributions in H_2: Calculation of rotational-vibrational preionization by multichannel quantum defect theory, J. Chim. Phys. **77**, 599 (1980).